Hardened state and binder efficiency of concrete produced with wastes of porcelain polishing and scheelite

C. Y. M. da Costa[1], A. G. de Medeiros[1], R. N. de Codes[2], M. T. Gurgel[3], F. J. N. de Lima[4]*

[1]*Federal Rural University of Semi-Arid, Department of Environmental Sciences and Engineering, Mossoró, RN, Brazil*
[2]*Federal Rural University of Semi-Arid, Department of Engineering and Technology, Mossoró, RN, Brazil*
[3]*Federal Rural University of Semi-Arid, Department of Agricultural and Forestry Sciences, Mossoró, RN, Brazil*
[4]*University of São Paulo, Polytechnic School, Department of Civil Construction, São Paulo, SP, Brazil*

Abstract

Reducing Portland cement consumption in concrete compositions, managing industrial waste, and conserving natural resources are contemporary challenges to achieving sustainable development. One solution has been the utilization of these industrial wastes as partial replacements for Portland cement or aggregates in concrete production. Due to the significant variability of these wastes, further research on this topic is necessary. Therefore, this study aimed to evaluate the properties of concrete mixtures containing porcelain polishing residue (PPR), scheelite residue (SR), and different types of Portland cement. The physical, chemical, and mineralogical characteristics of the wastes were determined. The fresh and hardened properties of the concretes, as well as the analysis of environmental impact, in terms of carbon dioxide emissions related to binder consumption, were investigated. The results showed that the utilization of these wastes resulted in reductions in consistency, water absorption, porosity, and compressive strength at 28 days by up to 33%, 16%, 13%, and 7%, respectively. Furthermore, improvements in microstructure, binder index, and CO_2 index were observed. The wastes reduced the cement content and CO_2 emissions per cubic meter of concrete to achieve 1 MPa by up to 12%. These findings suggested that the utilization of these wastes may be a viable and sustainable alternative to reduce Portland cement consumption and mitigate the environmental impact of the concrete industry. However, further research and studies are needed to assess other aspects, such as long-term durability and economic feasibility before their widespread adoption in the construction industry.

Keywords: pozzolanic activity, porosity, mechanical properties, microstructure, sustainability.

INTRODUCTION

The recent data presented at COP26 (United Nations Climate Conference), held in 2021 in Glasgow, Scotland, showed that more than half of CO_2 emissions (52.7%) occurred in the last 30 years [1]. As a result, according to the global climate report [2], the year 2020 was the second-hottest on record in the last 141 years, with an average global temperature variation of 0.98 °C. The land and ocean surface temperature in the Northern Hemisphere in 2020 was also the highest, at 1.28 °C above average, while in the Southern Hemisphere, it was the fifth-highest on record. The main effect of global warming felt by the world population has been climate change. In July 2021, deadly floods occurred in Germany and Belgium, causing destruction or severe damage to buildings and infrastructures such as bridges, sewage systems, schools, and hospitals [3]. In the previous month, the Pacific Northwestern region of the United States and Canada, known for their cold climates, experienced near-surface air temperature anomalies of 16-20 °C above normal, with the highest temperature recorded in Lytton with 49.6 °C for several days [4]. On the other hand, the Southern Hemisphere suffered from freezing temperatures, such as in cities in Southern Brazil, which reached their lowest temperatures in recent years [5]. It is natural to ask where all these emissions come from. According to the IPCC (Intergovernmental Panel on Climate Change) [6], which shows data on the main sources of CO_2 emissions in the world in megatons over the last 60 years, about 72% of carbon dioxide emissions in 2020 came from the burning of fossil fuels (oil and coal) to produce energy and materials, and 4.7% was derived from the production of Portland cement for construction.

The construction industry is a huge market that demands a large consumption of raw materials and energy for the manufacture of its materials, the main one being concrete. According to Andrew [7], global production of cement is the third-largest source of anthropogenic emissions of carbon dioxide, after fossil fuels and land-use change. Emissions that have intensified since 1990. Portland cement is a major environmental villain due to the amount of clinker used in its production. It is estimated that cement production emits between 800 [8] and 1150 [9] kg CO_2/t of clinker. This variation is mainly associated with the clinker content present in the cement in accordance with NBR 16697/2018 standard [10], which allows a minimum content between 25% and 45%. To collaborate with environmental sustainability, one of the several consolidated strategies to reduce CO_2 emissions from clinker production is the use of

*https://orcid.org/0000-0002-3893-2183

supplementary cementitious materials (SCMs). Currently, it has become common to use the following SCMs: metakaolin, natural pozzolans, limestone filler, fly ash, blast furnace slag, silica fume, rice husk ash, sugar cane bagasse ash, etc., in association with Portland cement, by promoting filler effect and/or reacting with the active constituents of the binder [11-16]. The use of such materials in concrete compositions, mixed with clinker during manufacture, or added separately during mixtures of cementitious products, results in a significant decrease in the amount of CO_2 released into the atmosphere. This result was verified in a study conducted in the United Kingdom, where the increase in the amount of SCMs resulted in a decrease in CO_2 release, including transportation of cement constituents [17].

Brazil has a vast availability of mineral resources and therefore, it has many industries that exploit such resources, generating significant amounts of waste at the end of the exploration process. For example, the exploration of scheelite in the Seridó Region in Northeast Brazil generates voluminous piles of waste in open-air banks, causing environmental damage. Another example is the ceramic industry for internal and external wall finishing, where the polishing process of porcelain tiles also generates a significant amount of waste [18, 19]. Carvalho et al. [20] found that the scheelite residue (SR) presents chemical, particle size, and mineralogical homogeneity, and therefore, it can replace natural sand in concrete. Pelisser et al. [21] and Breitenbach et al. [22] found that the porcelain polishing residue (PPR) has a particle size distribution similar to that of Portland cement and a chemical composition that is susceptible to developing pozzolanic activity, making it a potential replacement for Portland cement in concrete manufacturing. Also, according to the authors [23, 24], the filler effect provided by the fine grains of PPR improves the packing of cement particles and reduces porosity and permeability. Given the above, this paper aims to contribute to the sustainable development of concrete production by using residues from the polishing of porcelain tiles and scheelite in concrete with different types of cement to reduce the environmental impact related to CO_2 emissions, maintaining the binder index and compressive strength.

MATERIALS AND METHODS

Materials: two types of Portland cements that comply with NBR 16697/2018 standard [10], namely CP II Z-32-RS and CP V ARI-RS, natural sand, granitic gravel (GG), porcelain polishing residue (PPR), and scheelite residue (SR) were utilized. Raw PPR samples were collected from a ceramic factory (Elizabeth) located in the city of Conde in the State of Paraíba, Brazil. The samples were then dried at 70 °C for 24 h and ground in a ball mill for 40 min. Subsequently, the PPR fraction with a particle size <75 μm was selected to obtain a material with a particle size similar to that of cement. The SR was obtained from a tungsten mining company (Tomaz Salustino) located in the Seridó Region, State of Rio Grande do Norte, Brazil, and used as received. The physical characteristics of the materials are presented in Table I. The setting time of the cement paste was determined according to the procedure of NBR 16607:2018 standard [25]. The particle size distributions of GG, natural sand, and SR residue are shown in Fig. 1. The physical characterization revealed that the key differences between CP V and CP II cements were setting time, early-age compressive strength, and surface area. These variations arose from the fact that CP V is the finest among Brazilian Portland cements. In comparison, PPR differed from the cements in terms of surface area, which was 50% higher, and specific gravity, which was 21% lower. Sand and SR exhibited minimal differences between them.

Table II presents the chemical compositions in the form of oxides of CP II, CP V, and PPR. The quantification of

Table I - Physical characteristics of materials.

Characteristic	CP II	CP V	PPR	Sand	GG	SR
Residue #0.075 mm (%)	2.40	1.20	-	-	-	-
Initial set (min)	80	75	-	-	-	-
Compressive strength, 3 and 1 days* (MPa)	14.36	16.26	-	-	-	-
Compressive strength, 7 and 3 days* (MPa)	22.42	24.17	-	-	-	-
Compressive strength, 28 and 7 days* (MPa)	32.81	34.19	-	-	-	-
Specific surface area (cm^2/g)	3806	4688	8741	-	-	-
Specific gravity (g/cm^3)	2.99	3.06	2.39	2.59	2.67	2.94
Fineness modulus	-	-	-	2.63	6.64	1.99
Maximum dimension (mm)	-	-	-	2.36	19.00	2.36
Swelling coefficient	-	-	-	1.16	-	-
Absorption (%)	-	-	-	-	0.64	-

**: compressive strength ages for, respectively, cements CP II-Z-32-RS and CP V ARI-RS, according to [10].*

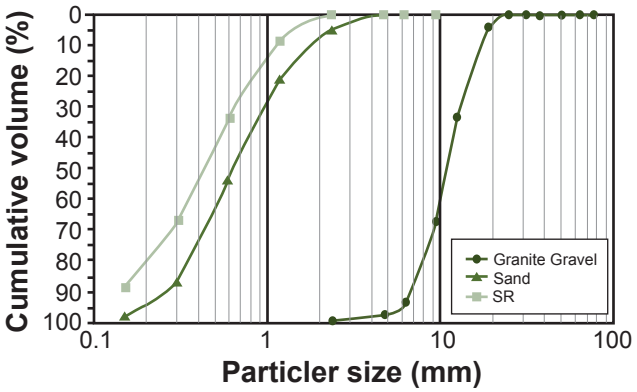

Figure 1: Particle size distribution curves of raw materials.

Table II - Chemical compositions (wt%) of fine materials.

Oxide	CP II	CP V	PPR	SR
CaO	48.77	58.00	1.06	34.14
SiO_2	26.12	19.06	61.84	30.64
Al_2O_3	10.93	7.92	22.04	13.01
MgO	4.32	4.72	6.86	-
SO_3	2.81	2.04	<0.10	-
Fe_2O_3	2.63	3.90	0.78	6.66
K_2O	0.97	1.06	3.74	1.09
TiO_2	0.30	0.23	0.15	0.49
MnO	0.20	0.18	0.13	0.64
WO_3	-	-	-	0.14
Others	<0.10	<0.10	0.12	0.29
LOI	2.93	2.87	3.28	12.96
Total	100	100	100	100

LOI: loss on ignition.

chemical species was obtained by X-ray fluorescence spectrometry using a spectrometer (EDX-7000, Shimadzu) with a maximum acceleration voltage of 50 kV. The loss on ignition followed the requirements of NBR NM 18:2012 standard [26]. Chemical analysis showed that the main constituents of Portland cements were oxides of calcium, silicon, aluminum, magnesium, and iron. However, CP II cement differed from CP V in terms of alumina content and CaO/SiO_2 ratio due to the addition of pozzolanic material. PPR can be considered a pozzolanic material, as the ASTM C618:2022 standard [27] establishes that the sum of $SiO_2+Al_2O_3+Fe_2O_3$ must be ≥70% and, in this case, it was equal to 84.7%. It should be noted that this standard classifies the material as pozzolanic based on the weight of these oxides without considering their reactivity. In SR the main constituents were oxides of calcium, silicon, aluminum, and iron.

Fig. 2 shows the X-ray diffraction (XRD) patterns of the RPP and RS samples, as well as the identified mineralogical phases. A diffractometer (LAB X XRD 6000, Shimadzu) was used for XRD analysis, operating with copper radiation and 2θ scanning at a rate of 2 °/min in the range of 10° to 80°. The main crystalline phases of SR were quartz, berlinite, dolomite, calcite, and magnetite, and those of PPR were quartz and mullite. The element K, present in the chemical composition of PPR, was not detected as a compound in the XRD pattern, leading to the conclusion that it was present as a substitutional element in mullite, which is used in glass production. Likewise, the elements Fe and Mg were also not identified as compounds in the XRD patterns, most likely because they were solved in a glassy phase, given the presence of an amorphous halo in the diffractogram between 15° and 35° of 2θ. This amorphous halo indicated that PPR can develop pozzolanic activity. The pozzolanic potential of PPR was also monitored by three different methods: i) NBR 5752:2014 [28]: the pozzolanic activity index resulted in 103%; ii) NBR 15895:2010 - modified Chapelle method [29]: fixed calcium content of 574 of mg $Ca(OH)_2$/g material; and iii) electrical conductivity method proposed by Luxán et al. [30]: the difference in electrical conductivity between the initial measurement and at 120 s was 0.46 mS/cm. According to these results, PPR can be considered a moderate pozzolanic material.

Composition of concretes: Fig. 3 presents the mass of each material necessary to produce 1 m^3 of concrete for the mix design 1:1.65:2.2:0.4. The concretes named REF CP II and REF CP V represented reference concretes produced without any residues, differing solely in the type of cement used. The concretes named C80/15 CP II and C80/15 CP V corresponded to the concretes produced with SR and PPR. The number 80 indicates that 80% of the mass of natural sand was substituted with SR, and the number 15 indicates that 15% of the mass of Portland cement was substituted with PPR. To maintain the proportion of fine:water ratio constant, a high-performance superplasticizer additive with a density of 1.08 g/cm^3 was used. The composition of concretes was based on a previous study [31], which utilized an optimization process of materials' granulometry and properties in the hardened state to determine the optimal levels of substitution as approximately 80 wt% of natural

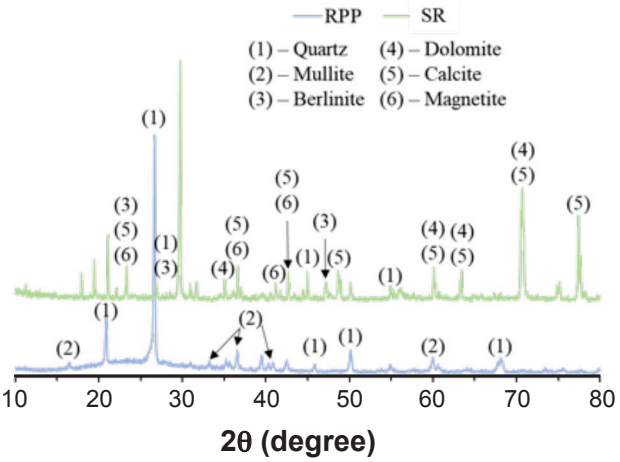

Figure 2: X-ray diffractograms of porcelain polishing residue (PPR) and scheelite residue (SR).

sand by SR and 15 wt% of Portland cement by PPR. The addition of superplasticizer (0.5 wt% of fine materials - Portland cement+PPR) and a fixed mortar content (α, Eq. A) of 43% were maintained for all concretes. The mortar content is a parameter that indirectly estimates the mobility of particles and provides the desired workability in terms of slump. In Eq. A, 'a' represents the amount of fine aggregate in mass, while m represents the sum of coarse and fine aggregate in mass:

$$\alpha = \frac{1 + a}{1 + m} \quad (A)$$

Concrete mixture: the concretes were produced in a 120 L capacity mechanical mixer, following the procedure shown in Fig. 4. For the mixture of concretes with residues, PPR and SR were previously mixed with cement and sand. Twelve cylindrical specimens, each with a diameter of 20 cm and a height of 10 cm, were produced for each concrete, totaling 48 specimens. Metallic molds were used, which were coated with lubricant on the surface, and manual densification was performed every 1/3 of the volume's capacity. The specimens were kept in the molds for 24 h and were stored in a covered and closed place at room temperature. They were then de-molded and identified, and placed in a tank with a saturated calcium hydroxide solution for curing until the required age for testing [32].

Fresh state properties: the evaluated fresh state properties were the specific mass, according to ABNT NBR 9833:2008 [33], and the workability, which was assessed through the slump cone test, in accordance with ABNT NBR 16889:2020 [34]. The slump test is the most used method for evaluating the flow properties of fresh concrete, as it is easy to perform and inexpensive. The slump test equipment consists of a truncated cone and a measuring device, such as a ruler. The slump is measured by taking the difference between the height of the truncated cone at the beginning of the test and after the flow has stopped. Although slump is a qualitative evaluation of the workability of the mixture, the test measurements can be related to the yield stress of the material under low shear rates [35]. The yield stress is a unique property of the material that best describes the behavior of fresh concrete and is usually determined by rotational or oscillatory rheometric tests. In these tests, it is assumed that the fresh behavior of cementitious suspensions, such as concrete, is fluid with yield stress and can be approximated by the Herschell-Bulkley model [36]. This allows for the evaluation of the flow behavior of the material simulating the different rheological situations, such as mixing, transport, and application. A viable alternative for determining the yield stress of concrete is to use the Roussel

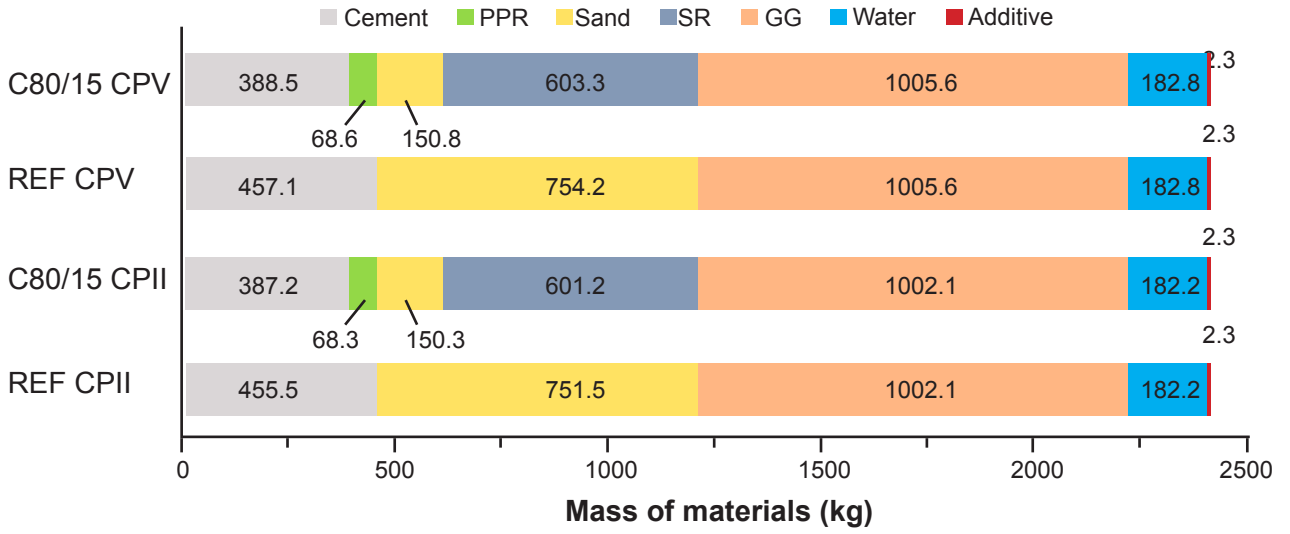

Figure 3: Material consumptions (kg) for 1 m^3 of concrete.

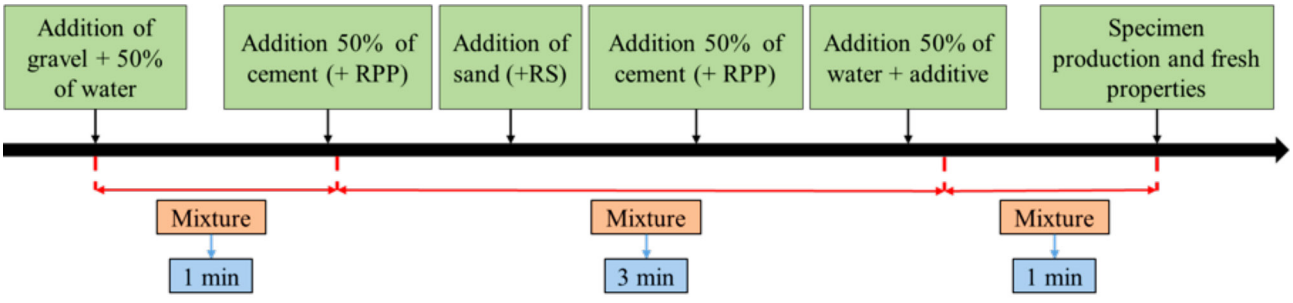

Figure 4: Schematic of concrete mixing procedure.

model [37], which relates yield stress, slump, and specific mass by:

$$S = 25.5 - \frac{17.6\tau}{\rho} \quad (B)$$

where S is the slump (cm), τ is the yield stress (Pa), and ϱ is the specific mass (kg/m^3). This equation is valid for slumps between 5 and 25 cm.

Hardened state properties: in the hardened state, the absorption and porosity [38], capillary absorption [39], axial compressive strength [40], ultrasound testing [41], and scanning electron microscopy (SEM) were evaluated. All hardened state tests were performed at 28 days of curing. To measure the absorption and porosity, the dry mass (m_s) of the specimens was determined after drying in an oven at 100 °C for 24 h, as well as the saturation mass in water (m_{sat}) and the submerged mass in water (m_i). Eqs. C and D were used to determine absorption and porosity, respectively:

$$A(\%) = \frac{m_{sat} - m_s}{m_s} .100 \quad (C)$$

$$P(\%) = \frac{m_{sat} - m_s}{m_{sat} - m_i} .100 \quad (D)$$

For capillary absorption, cylindrical concrete specimens were placed in contact with a 5±1 mm layer of water. The face of the concrete cylinder in contact with water contained the matrix and visible aggregates to force water in and rise by capillary action. The mass gain of the sample was evaluated at 3, 6, 24, 48 and 72 h. The compressive strength test was conducted using a press (PC 200C, Emic) at a constant loading rate of 0.50 MPa/s. The ultrasound test was performed by direct transmission, according to NBR 8802:2019 and ACI 228.2R:2013 [41, 42], with a longitudinal wave transducer at a frequency of 54 kHz. The transducer and specimen interface were lubricated with medical ultrasound gel. The dynamic modulus of elasticity was calculated using Eq. E, with Poisson's ratio (ν) set to 0.2, as suggested by NBR 6118:2014 [43]:

$$E = \frac{[\rho(1+\nu)(1-2\nu)]\, V^2}{(1-\nu)} \quad (E)$$

where E is dynamic modulus of elasticity (GPa), ϱ is density (kg/m^3), and V is ultrasonic wave velocity (m/s). Scanning electron microscopy (SEM) was conducted using a microscope (Vega 3 LMU, Tescan). The samples were subjected to a cryogenic process in a bath with liquid nitrogen for 2 min, then cut into cubes of dimensions of 2x2x2 cm and subsequently dried in an oven at 105±5 °C for 24 h. The cubes were gold-plated with a 6 nm layer to increase the image contrast.

Estimation of environmental impact: it is known that the use of mineral additions in concrete, including industrial by-products, contributes to the reduction of CO_2 associated with the production of clinker. This strategy, combined with the efficient use of Portland cements, tends to further enhance this advantage [44]. In this research, the concrete efficiency was calculated according to the method developed by Damineli et al. [45], which relates the efficiency of concrete through the binder index (b_i) and CO_2 index (c_i) calculated by:

$$b_i = \frac{b}{p} \quad (F)$$

$$c_i = \frac{c}{p} \quad (G)$$

where b is the total consumption of Portland cement (kg/m^3), c is the total amount of CO_2 emitted during concrete manufacturing, and p is the compressive strength at 28 days (MPa). The b_i and c_i measure the total amount of Portland cement and the amount of CO_2 emitted for each 1 MPa of concrete strength, respectively. As such, the lower the b and c values, the more eco-efficient is the concrete mixture. Since the goal of this study is not to make an extensive and detailed life-cycle analysis of the cements used in this research, for simplification purposes, it was considered that for 1 ton of clinker, 1 ton of CO_2 was emitted [46-48]. It was also considered that, based on NBR 16697:2018 [10], CP II and CP V cements had 75% and 95% of clinker in their composition, respectively.

RESULTS AND DISCUSSION

Fresh state properties

Table III presents the results of the specific mass, slump, and yield stress of the concretes in the fresh state. When analyzing the specific mass of the concretes produced with wastes, it was noticed that the values were similar in comparison to the reference concretes, suggesting that the effects of the wastes were insignificant. However, when separately evaluating the specific mass of the materials used, it was possible to notice the influence of wastes in the process. The scheelite residue (SR), for example, presented a specific mass 12% higher than that of sand, while the porcelain polishing residue (PPR) presented a specific mass, on average, 21% lower than that of Portland cement. The combination of these residues resulted in an equalization that kept the specific mass of the concrete practically constant. Therefore, it can be concluded that even if the effects of isolated residues were not significant, they had an impact on the result when combined.

Table III - Properties of concrete in the fresh state.

Concrete	ϱ (g/cm^3)	S (mm)	τ (Pa)
REF CP II	2.40	100	2114
C80/15 CP II	2.44	75	2495
REF CP V	2.45	75	2506
C80/15 CP V	2.47	50	2877

ϱ*: specific mass; S: slump;* τ*: yield stress.*

The result of the concrete slump test is influenced by the physical characteristics of the materials, mortar content, and the amount of water present in the mixture [49]. As the last two parameters were kept constant, it was the physical characteristics of the materials that influenced the workability of the concretes. The C80/15 CP II and C80/15 CP V concretes showed a reduction of 25% and 44% in slump compared to the REF CP II and REF CP V concretes, respectively. This reduction was mainly caused by the PPR since the sand and SR had similar particle sizes. The PPR had a specific surface area that was 50% higher than that of the cements, so more water was needed to surround the grains. This reduction in the slump test was even more pronounced in the REF CP V and C80/15 CP V concretes due to the CP V cement, which also had a higher specific surface area than the CP II cement. In practical terms of workability, low, high, or intermediate slumps correspond to consistent or 'rough' concrete, flowable concrete, and workable concrete [50]. This means that the smaller the slump, the greater the flow resistance and the higher the yield stress, and conversely, the greater the slump, the lower the flow resistance and the lower the yield stress. Yield stress results confirmed this inverse relationship between slump and yield stress. The REF CP II concrete showed the highest slump and lower yield stress, and therefore, it flowed more easily than the C80/15 CP V concrete, which showed the lowest slump and highest yield stress. A similar result was obtained by Murata [51].

Hardened state

Water absorption and porosity by Archimedes' test: concretes with a compact structure and lower void rates have lower absorption, porosity, and permeability rates; consequently, they are less susceptible to pathologies, maintaining their service properties for a longer time. Therefore, absorption and porosity are important properties that directly influence the durability of concrete. Fig. 5 shows the results of water absorption and porosity determined by Archimedes' test of the concretes. It was noted that the type of Portland cement and the use of PPR and SR residues affected the absorption and porosity of the concretes. When comparing the concrete mixtures without residues, it was observed that REF CP V presented values of absorption and porosity approximately 23% higher than REF CP II concrete. This difference may have been caused using CP V cement, which had a specific surface area 23% greater than CP II cement. This can result in high rates of heat release during hydration reactions, causing the evaporation of water from the medium and an increase in the void ratio of the concrete. Furthermore, unlike CP II cement, CP V cement does not contain pozzolanic material in its composition, which may have contributed to the higher values of absorption and porosity observed.

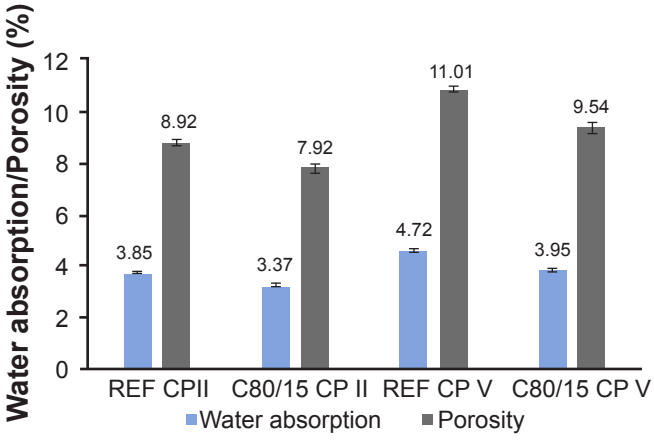

Figure 5: Water absorption and porosity by Archimedes' test.

When analyzing the concrete with residues, it was noted that the absorption and porosity of the C80/15 CP II concrete were lower by 12.5% and 11%, respectively, compared to REF CP II concrete. Similarly, the C80/15 CP V concrete showed a reduction of 16% and 13% in absorption and porosity, respectively, compared to REF CP V concrete. These reductions were caused by PPR, which had a filler effect (filling voids by physical action) and pozzolanic activity (filling pores by chemical action) [52]. Among all the concretes, C80/15 CP II had the lowest values of absorption and porosity, combining the effect of PPR and cement CP II. According to the technical bulletin CEB 192:1989 of the Euro-International Committee on Concrete [53], concrete can be qualitatively classified as good, medium, or bad, depending on the level of absorption by immersion. Fig. 6 shows the correlation between experimental data on Archimedes water absorption and the CEB 192:1989 classification. It can be observed that all concretes had an average quality based on the recorded absorption values.

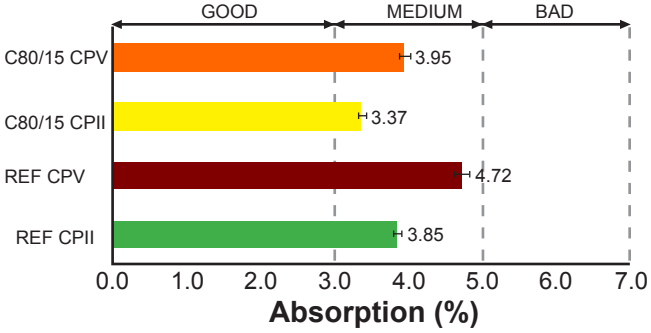

Figure 6: Water absorption by immersion and concrete quality according to CEB 192:1989 [53].

Water absorption by capillarity: the capillary absorption of concrete is an important characteristic that affects its strength and durability. As per Hall [54], the capillary absorption of porous materials, such as concrete, is directly proportional to the square root of time, as indicated by:

$$AC = S\sqrt{t} \qquad (H)$$

where the term AC is the capillary absorption (mg/mm^2), S is the absorption coefficient ($mg.mm^{-2}.min^{-0.5}$), and t is the time (min). Fig. 7 shows the levels of water absorption

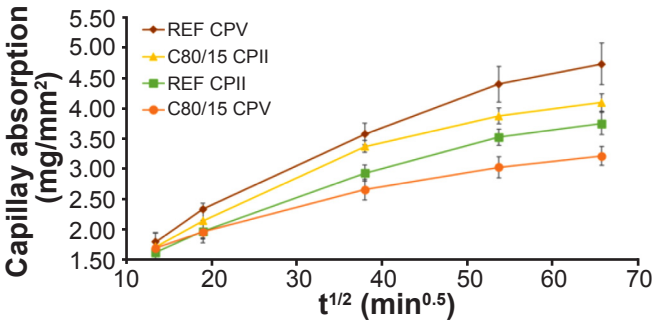

Figure 7: Water absorption by capillarity as a function of time$^{1/2}$.

by capillarity of the concretes as a function of the square root of time, according to Eq. H. In general, all concretes showed similar behavior, with a higher absorption rate during the first hours, followed by deceleration, as indicated by the slope of lines on the graph. This behavior is typical of concrete, where there is rapid capillary water absorption at the beginning of the test, followed by stabilization over time since the pores closest to the surface become saturated [55]. From Fig. 7, it is possible to observe that up to 6 h, capillary absorption was similar for all types of concrete. However, after 24 h, this characteristic began to exhibit significant differences. After 72 h, the capillary absorption of REF CP V concrete was 4.74 mg/mm^2, while that of C80/15 CP V was 3.22 mg/mm^2, representing a reduction of 32%. This reduction may be associated with the decrease in the average pore diameter due to the filling effect of the RPP residue. On the other hand, REF CP II concrete presented a capillary absorption of 3.76 mg/mm^2, while C80/15 CP II had an increase of 9%, with an absorption of 4.10 mg/mm^2. This increase may indicate that there was a greater amount of connected pores in C80/15 CP II concrete.

Based on the results obtained in Fig. 7, it was possible to determine the absorption coefficient (S) of the concretes.

Table IV - Classification of Browne and absorption coefficient (S) of concretes.

Concrete	S (mg.mm^{-2}.min$^{-0.5}$)
REF CP II	0.057
REF CP V	0.072
C80/15 CP II	0.062
C80/15 CP V	0.049

Browne's classification for concrete quality: S>0.2 (low), S=0.2-0.1 (medium), S<0.1 (high).

This parameter is related to the hydraulic diffusivity and represents the water penetration rate during the initial stages. The determination of the absorption coefficient is influenced by factors such as surface characteristics and the pressure difference between the free surface of the liquid and the surface of the same liquid inside the capillary [56]. Several authors use the absorption coefficient as an indicator of the quality of the concrete, and in this work, the classification proposed by Browne [57] was adopted. The values obtained for the absorption coefficients of the evaluated concretes are shown in Table IV. According to Browne's classification, the concretes had high quality. The incorporation of residues had no direct effects on the absorption coefficient, as this parameter depends more on the surface quality (smooth appearance and presence of pores). However, indirectly, it was observed that the RPP residue may have contributed to the reduction of the average pore diameter.

Mechanical properties: the results for specific mass in the hardened state, ultrasound pulse propagation velocity, modulus of elasticity, and compressive strength are presented in Table V. A comparison of the results of C80/15 CP II and C80/15 CP V concretes with the REF CP II and REF CP V concretes was made, analyzing their mechanical and microstructural properties. For concretes C80/15 CP II and C80/15 CP V, an increase of 1.6% and 4.9% in specific mass in relation to concretes REF CP II and REC CP V, respectively, was recorded. It was observed that the addition of residues contributed to the increase due to the filler effect of the RPP and the higher density of the RS in relation to the sand. This result also explained why concretes with residues performed better in durability tests. Another consequence is the probable reduction of voids, with a great influence on the quality and mechanical properties of the concrete.

The C80/15 CP II and C80/15 CP V concretes showed a 2% higher propagation speed of the ultrasonic pulse than the concretes without residues, due to the reduction of porosity. Therefore, it is presumable that these concretes had better quality. However, the classification of IS 13133-1:1992 standard [58] states that concretes with ultrasonic pulse propagation velocity above 4500 m/s are considered of excellent quality. This qualitative classification provides little information about the influence of materials and places all concretes at the same level of quality. To complement the information, the ASTM C597:2016 standard [59] was used, which considers the intrinsic characteristics of the materials and the concrete production process. According to this standard, higher ultrasonic pulse propagation velocities

Table V - Mechanical properties of concrete at 28 days.

Concrete	ϱ (kg/m^3)	V (m/s)	E (GPa)	CS (MPa)
REF CP II	2317±5	4648±5	45.04±0.04	40.6±0.7
C80/15 CP II	2348±11	4751±32	47.70±0.82	36.7±0.9
REF CP V	2275±8	4573±13	42.82±0.25	48.8±0.5
C80/15 CP V	2386±6	4682±44	47.08±0.79	47.3±1.1

ϱ*: specific mass; V: ultrasound pulse propagation velocity; E: modulus of elasticity; CS: compressive strength.*

are common in concrete with greater uniformity and better relative quality, while lower velocities indicate concrete with cracks or voids. Thus, it is possible to state that concrete with waste had better quality and greater uniformity. The positive effect on mechanical properties was that the dynamic modulus of elasticity of concretes C80/15 REF II and C80/15 CP were approximately 6% and 10% higher than concretes REF CP II and REF CP V, respectively. Sing and Siddique [60] state that the increase in the modulus of elasticity promotes greater stiffness in the material, allowing it to undergo greater stresses with less deformation, contributing to a better performance of structures.

Considering that the C80/15 CP II and C80/15 CP V concretes showed better quality, lower porosity, and higher modulus of elasticity, higher compressive strength was also expected. However, the results showed that the compressive strength of the REF CPV and C80/15 CP V concretes were statistically equal and that of the REF CP II concrete was 10.7% higher than the C80/15 CP II concrete. To corroborate the results, Salvi et al. [61] concluded that the use of porcelain polishing residue between 20% and 40% in concrete promoted the reduction of the compressive strength in up to 28 days of curing, due to the replacement of the hydraulic bonding material by other non-hydraulic ones. In some cases, there was an increase when the curing time was longer than 90 days, attributed to pozzolanic activity. This result shows that predicting the compressive strength of concrete based on the porosity value is not enough; it is necessary to consider the pore structure, pore size, pore connectivity, and pore distribution. The pore structure has a great influence on the compressive strength [62].

In addition to the pore structure, other factors may have influenced the strength of the concrete. Three of the possible causes of this result are: first is the reduction of the cement content using PPR residue, second is the changes in the microstructure formed (Fig. 8), and third is the length of the transition zone. The microstructure of the concretes is shown in Fig. 8 at different magnifications. In the images, it can be seen that the REF CP II concrete (Fig. 8a) had a shorter transition zone length and smaller amount and size of pores, and the REF CP V concrete (Fig. 8b) had a higher amount of hydrated calcium silicate (C-S-H). Concrete C80/15 CP II (Fig. 8c) and C80/15 CP V (Fig. 8d) showed crystalline structure of C-S-H with micropores. These micropores had a smaller diameter and were better distributed, which must have contributed to lower porosity, water absorption by Archimedes, and capillarity. The use of PPR and SR in concrete mixtures resulted in a more compact and less porous microstructure. These changes in microstructure can have a positive effect on the overall performance of concrete since they are intrinsically related to compressive strength and mass transport throughout the microstructure [63].

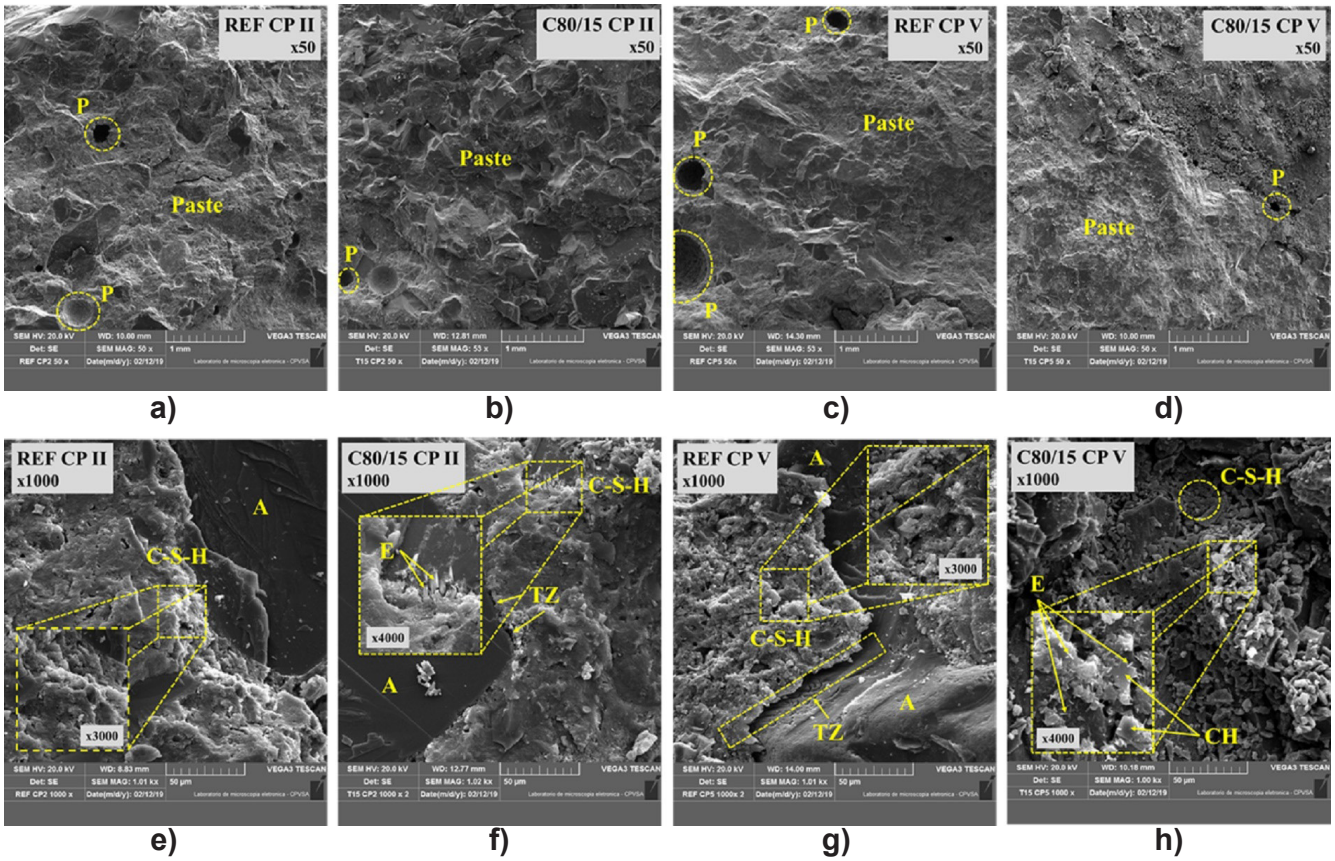

Figure 8: SEM micrographs of concretes: a,e) REF CP II; b,f) C80/15 CP II; c,g) REF CP V; and d,h) C80/15 CP V (P - pore; C-S-H - hydrated calcium silicate; A - aggregate; TZ - transition zone; E - ettringite; CH - portlandite).

Analysis of the environmental impact

Table VI shows the calculated binder index (b_i) and estimated CO_2 index (c_i) of the concretes, while Fig. 9 shows a plot of these coefficients by compressive strength at 28 days. The use of CP V cement improved the efficiency in terms of b_i due to the high initial resistance, however, the same efficiency in terms of c_i was not seen, because the amount of clinker in its composition was higher. The use of CP II cement had an inverse relationship, with greater efficiency in c_i than in b_i. The incorporation of residues showed to be an advantageous alternative to improve the efficiency of the C80/15 CP II and C80/15 CP V concretes; in comparison with the reference concretes, an increase of 8.6% and 12.8% in the efficiency in terms of b_i and an increase of 8.0% and 12.4% in terms of c_i, respectively, were observed.

By observing Fig. 9, the concretes REF CP II and REF CP V had roughly the same binder consumption per m^3, and this consumption was higher than the concretes C80/15 CP II and C80/15 CP V, as they were closer to the consumption line of 500 kg/m^3. Concrete REF CP V exhibited the worst efficiency in terms of c_i and concrete C80/15 CP II had the lowest compressive strength. Therefore, concrete C80/15 CP V demonstrated the best environmental efficiency in terms of b_i, c_i, and compressive strength. The Brazilian standard NBR 12655:2022 [64] requires a minimum Portland cement consumption for structural concrete of 260 kg/m^3 for low environmental aggressiveness class and up to 360 kg/m^3 for strong environmental aggressiveness to ensure durability. However, according to the results presented here and the research of Wassermann et al. [65], the durability indicators are not affected when the Portland cement content is reduced to within the limits investigated. On the contrary, it was observed that by increasing particle packing density by using alternative materials, improvements in mechanical properties, microstructure, and durability were obtained.

Table VI - Calculated binder index (b_i) and estimated CO_2 index (c_i) of concretes.

Concrete	b_i (kg.m^{-3}.MPa^{-1})	c_i (kg.m^{-3}.MPa^{-1})
REF CP II	11.60	8.70
C80/15 CP II	10.60	8.00
REF CP V	9.40	8.90
C80/15 CP V	8.20	7.80

CONCLUSIONS

The results indicated that the use of scheelite residue (SR) and porcelain polishing residue (PPR) in the production of concrete caused a reduction in consistency of up to 44%. However, they contributed to significant improvements in physical properties, increasing specific mass by up to 5%, and durability, reducing porosity and water absorption by up to 13% and 16%, respectively. Part of these improvements was a consequence of the better packing of the particles with the SR and the combination of the filler effect with the pozzolanic potential of the PPR. Although there was a small reduction in the compressive strength at 28 days, the concretes with residues presented higher estimated stiffness and a more compact and less porous microstructure. In addition, the use of SR and PPR achieved the sustainability objective, as it improved the environmental efficiency of concrete in terms of CO_2 reduction related to binder index and compressive strength. Overall, these findings support the incorporation of SR and PPR in concrete production to improve performance and sustainability.

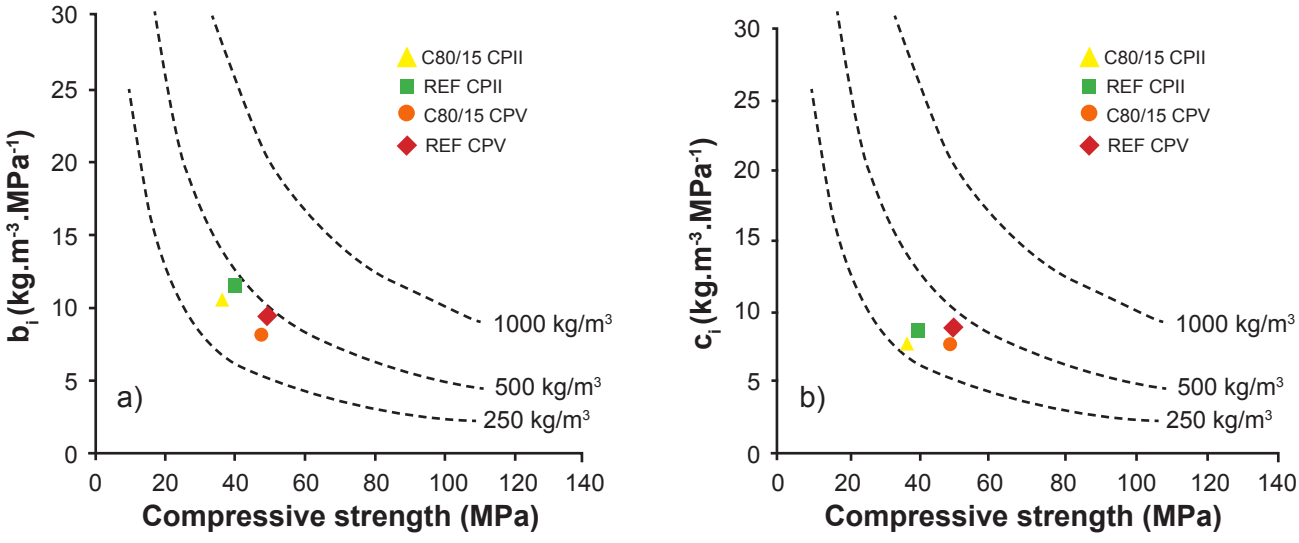

Figure 9: Binder index, b_i (a), and CO_2 index, c_i (b), versus compressive strength at 28 days. The dotted lines represent concretes with the same amount of binder and total CO_2.

ACKNOWLEDGEMENT

The authors are grateful for the support of the Federal Rural University of Semi-Arid.

REFERENCES

[1] COP26, "Outcomes", UN Clim. Change Conf. (2021) //ukcop26.org, acc. 16/01/2022.
[2] ACNUDH, "Mudanças climáticas e direitos humanos: um clima seguro" (2019) www.ohchr.org, acc. 16/01/2022.
[3] S. Mohr, U. Ehret, M. Kunz, P. Ludwig, A. Caldas-Alvarez, J.E. Daniell, F. Ehmele, H. Feldmann, M.J. Franca, C. Gattke, M. Hundhausen, P. Knippertz, K. Küpfer, B. Mühr, J.G. Pinto, J. Quinting, A.M. Schäfer, M. Scheibel, F. Seidel, C. Witsozky, Nat. Hazards Earth Syst. Sci. **23** (2023) 525.
[4] R.H. White, S. Anderson, J.F. Booth, G. Braich, C. Draeger, C. Fei, C.D.G. Harley, S.B. Henderson, M. Jakob, C.A. Lau, L.M. Admasu, V. Narinesingh, C. Rondell, E. Roocoft, K.R. Weinberger, G. West, Nat. Commun. **14** (2023) 1.
[5] J. Marengo, J.C. Espinoza, L. Bettolli, A.P. Cunha, J. Molina-Carpio, M. Skansi, K. Correa, A.M. Ramos, R. Salinas, J.-P. Sierra, Clim. Dynam. **60** (2023) 23.
[6] IPCC, Intergov. Panel Clim. Change, ipcc.ch/, acc. 24/03/2022.
[7] R.M. Andrew, Earth Syst. Sci. Data **11** (2019) 1675.
[8] A. Josa, A. Aguado, A. Heino, E. Byars, A. Cardim, Cem. Concr. Res. **34** (2004) 1313.
[9] J.K. Yamamoto, Y. Kihara, A.M. Coimbra, T.J. Montanheiro, Environ. Geosci. **4** (1997) 192.
[10] ABNT, NBR 16697, "Cimento Portland: requisitos" Ass. Bras. Normas Técn., S. Paulo (2018).
[11] I.G. Richardson, A.V. Girão, R. Taylor, S. Jia, Cem. Concr. Res. **83** (2016) 1.
[12] K. Scrivener, F. Martirena, S. Bishnoi, S. Maity, Cem. Concr. Res. **114** (2018) 17.
[13] K.L. Scrivener, V.M. John, E.M. Gartner, Cem. Concr. Res. **114** (2016) 2.
[14] K.L. Scrivener, R.J. Kirkpatrick, Cem. Concr. Res. **38** (2008) 128.
[15] V.M. John, B.L. Damineli, M. Quattrone, R.G. Pileggi, Cem. Concr. Res. **114** (2018) 65.
[16] R. Siddique, J. Klaus, Appl. Clay Sci. **43** (2009) 392.
[17] B. Lothenbach, K. Scrivener, R.D. Hooton, Cem. Concr. Res. **41** (2011) 1244.
[18] A. Singh, V. Srivastava, in Proc. Recent Adv. Eng. Technol. Comput. Sci., IEEE (2018).
[19] P.C. Jacoby, F. Pelisser, J. Clean. Prod. **100** (2015) 84.
[20] E.B. Carvalho, R.F.S. Lima, R.A. Petta, J.B.A. Paulo, L.C. Souza, in 19th Enc. Nac. Trat. Min. Met. Extrat., Recife (2002) 75.
[21] F. Pelisser, N. Zavarise, T.A. Longo, A.M. Bernardin, J. Clean. Prod. **19** (2011) 757.
[22] S.B. Breitenbach, O.C. Santos, J.C.S. Andrade, R.M. Nascimento, A.E. Martinelli, Cerâmica **63** (2017) 395.
[23] C.S.G. Penteado, E.V. de Carvalho, R.C.C. Lintz, J. Clean. Prod. **112** (2016) 514.
[24] L.R. Steiner, A.M. Bernardin, F. Pelisser, Sust. Mater. Technol. **4** (2015) 30.
[25] ABNT, NBR 16607, "Cimento Portland: determinação dos tempos de pega", Ass. Bras. Normas Técn., S. Paulo (2018).
[26] ABNT, NBR NM 18, "Análise química: determinação de perda ao fogo", Ass. Bras. Normas Técn., S. Paulo (2012).
[27] ASTM, C618, "Standard specification for coal fly ash and raw or calcined natural pozzolan for use in concrete", Amer. Soc. Test. Mater. (2022).
[28] ABNT, NBR 5752, "Materiais pozolânicos: determinação do índice de desempenho com cimento Portland aos 28 dias", Ass. Bras. Normas Técn., S. Paulo (2014).
[29] ABNT, NBR 15895, "Materiais pozolânicos: determinação do teor de hidróxido de cálcio fixado, método Chapelle modificado", Ass. Bras. Normas Técn., S. Paulo (2010).
[30] M.P. Luxán, F. Madruga, J. Saavedra, Cem. Concr. Res. **19** (1989) 63.
[31] A.G. Medeiros, M.T. Gurgel, W.G. da Silva, M.P. de Oliveira, R.L.S. Ferreira, F.J.N. de Lima, Constr. Build. Mater. **296** (2021)123719.
[32] ABNT, NBR 5738, "Concreto: procedimento para moldagem e cura de corpos de prova", Ass. Bras. Normas Técn., S. Paulo (2016).
[33] ABNT, NBR 9833, "Concreto fresco: determinação da massa específica, do rendimento e do teor de ar pelo método gravimétrico", Ass. Bras. Normas Técn., S. Paulo (2008).
[34] ABNT, NBR 16889, "Concreto: determinação da consistência pelo abatimento do tronco de cone", Ass. Bras. Normas Técn., S. Paulo (2020).
[35] J. Hoppe Filho, M.A. Cincotto, R.G. Pileggi, Concr. Constr. **34** (2007) 108.
[36] K. Kovler, N. Roussel, Cem. Concr. Res. **41** (2011) 775.
[37] N. Roussel, Mater. Struct. **39** (2006) 501.
[38] ABNT, NBR 9778, "Argamassa e concretos endurecidos: determinação da absorção de água, índice de vazios e massa específica", Ass. Bras. Normas Técn., S. Paulo (2009).
[39] ABNT, NBR 9779, "Argamassas e concretos endurecidos: determinação da absorção de água por capilaridade", Ass. Bras. Normas Técn., S. Paulo (2012).
[40] ABNT, NBR 5739, "Concreto: ensaio de compressão de corpos de prova cilíndricos", Ass. Bras. Normas Técn., S. Paulo (2018).
[41] ABNT, NBR 8802, "Cimento endurecido: determinação da velocidade de propagação de onda ultrassônica", Ass. Bras. Normas Técn., S. Paulo (2019).
[42] ACI, 228.2R, "Nondestructive test methods for evaluation of concrete in structures", Am. Concr. Inst. (2013).
[43] ABNT, NBR 6118, "Projeto de estruturas de concreto: procedimento", Ass. Bras. Normas Técn., S. Paulo (2014).
[44] J.S. Damtoft, J. Lukasik, D. Herfort, D. Sorrentino, E.M. Gartner, Cem. Concr. Res. **38** (2008) 115.

[45] B.L. Damineli, F.M. Kemeid, P.S. Aguiar, V.M. John, Cem. Concr. Compos. **32** (2010) 555.
[46] P.R. de Matos, R.D. Sakata, L.R. Prudêncio, Constr. Build. Mater. **225** (2019) 941.
[47] L. Barcelo, J. Kline, G. Walenta, E. Gartner, Mater. Struct. **47** (2014) 1055.
[48] W. Shen, L. Cao, Q. Li, W. Zhang, G. Wang, C. Li, Renew. Sustain. Energy Rev. **50** (2015) 1004.
[49] B.L. Damineli, R.G. Pileggi, V.M. John, Rev. Ibracon Estrut. Mater. **10** (2017) 998.
[50] A.W. Saak, H.M. Jennings, S.P. Shah, Cem. Concr. Res. **34** (2004) 363.
[51] J. Murata, Matér. Const. **17** (1984) 117.
[52] Z.L.M. Sampaio, A.E. Martinelli, T.S. Gomes, Cerâmica **63**, 368 (2017) 530.
[53] CEB, 192, "Diagnosis and assessment of concrete structures", Commit. Euro-Inter. Beton (1989).
[54] C. Hall, Mag. Concr. Res. **41** (1989) 51.
[55] J. Nobre, M. Bravo, J. de Brito, G. Duarte, J. Build. Eng. **29** (2020) 101135.
[56] D.O.J. dos Santos, C.M.A. Fontes, P.R.L. Lima, Matéria **22** (2017) 11801.
[57] R.D. Browne, "Field investigations, site and laboratory tests: maintenance repair and rehabilitation of concrete structures", CEEC, Lisbon (1991).
[58] IS, 13133, "Methods of non-destructive testing of concrete: part 1 ultrasonic pulse velocity", Bur. Ind. Stand. (1992).
[59] ASTM, C597, "Standard test method for pulse velocity through concrete", Amer. Soc. Test. Mater. (2016).
[60] G. Singh, R. Siddique, Constr. Build. Mater. **26** (2012) 416.
[61] D. Salvi, T. Gupta, R.K. Sharma, J. Sci. Res. Rep. **27** (2021) 87.
[62] D. Li, Z. Li, C. Lv, G. Zhang, Y. Yin, Constr. Build. Mater. **170** (2018) 520.
[63] H.F.W. Taylor, *Cement chemistry*, 2nd ed., Thomas Telford, London (1997).
[64] ABNT, NBR 12655, "Concreto de cimento Portland: preparo, controle, recebimento e aceitação; procedimentos", Ass. Bras. Normas Técn., S. Paulo (2022).
[65] R. Wassermann, A. Katz, A. Bentur, Mater. Struct. **42** (2009) 973.
(Rec. 20/02/2023, Rev. 25/05/2023, Ac. 12/07/2023)